Inácio de Carvalho, V., de Carvalho, M., Alonzo, T. A., and González-Manteiga, W. (2016+), "Functional Partial Area under the Curve Regression with an Application to Metabolic Syndrome Diagnosis," Annals of Applied Statistics, in press.

Submitted to the Annals of Applied Statistics

FUNCTIONAL COVARIATE-ADJUSTED PARTIAL AREA UNDER THE SPECIFICITY-ROC CURVE WITH AN APPLICATION TO METABOLIC SYNDROME DIAGNOSIS (SUPPLEMENTARY MATERIAL)

By Vanda Inácio de Carvalho, Miguel de Carvalho, Todd A. Alonzo and Wenceslao González-Manteiga

Pontificia Universidad Católica de Chile, University of Southern California† and Universidade de Santiago de Compostela‡*

1. Auxiliary results.

1.1. *Population specificity-ROC curve and partial area under the curve.* Here we show that the survival distribution of the covariate-dependent random variable $Z_X = S_D(Y_{\bar{D}} \mid X) = 1 - F_D(Y_{\bar{D}} \mid X)$ is the $\mathrm{ROC}_{\mathrm{Sp}}(p \mid X)$ curve, where

$$\mathrm{ROC}_{\mathrm{Sp}}(p \mid X) = F_{\varepsilon_{\bar{D}}}\left\{\frac{\mu_D(X) - \mu_{\bar{D}}(X)}{\sigma_{\bar{D}}(X)} + \frac{\sigma_D(X)}{\sigma_{\bar{D}}(X)} F^{-1}_{\varepsilon_D}(1-p)\right\}, \quad 0 \leqslant p \leqslant 1.$$

By definition, for $0 \leqslant p \leqslant 1$,

$$S_{Z_X}(p \mid X) = \Pr(Z_X \geqslant p \mid X) = \Pr(Y_{\bar{D}} \leqslant S^{-1}_D(p \mid X) \mid X) = \Pr(Y_{\bar{D}} \leqslant F^{-1}_D(1-p \mid X) \mid X).$$

As a consequence of assuming a location–scale regression model for Y_D and $Y_{\bar{D}}$, we have

$$F^{-1}_D(1-p \mid X) = \mu_D(X) + \sigma_D(X) F^{-1}_{\varepsilon_D}(1-p),$$

where $F^{-1}(1-p) = \inf\{x \in \mathbb{R} : F(x) \geqslant 1-p\}$. Thus, it is trivial to conclude that

$$\begin{aligned} S_{Z_X}(p \mid X) &= \Pr(\mu_{\bar{D}}(X) + \sigma_{\bar{D}}(X)\varepsilon_{\bar{D}} \leqslant \mu_D(X) + \sigma_D(X) F^{-1}_{\varepsilon_D}(1-p)) \\ &= F_{\varepsilon_{\bar{D}}}\left\{\frac{\mu_D(X) - \mu_{\bar{D}}(X)}{\sigma_{\bar{D}}(X)} + \frac{\sigma_D(X)}{\sigma_{\bar{D}}(X)} F^{-1}_{\varepsilon_D}(1-p)\right\} \\ &= \mathrm{ROC}_{\mathrm{Sp}}(p \mid X). \end{aligned}$$

We now show that

$$\mathrm{pAUC}_{\mathrm{Se}}(u \mid X) = \int_u^1 \mathrm{ROC}_{\mathrm{Sp}}(p \mid X)\, \mathrm{d}p = \mathrm{E}[\max\{u, Z_X\} \mid X] - u. \tag{1.1}$$

First, note that integrating by parts we have

$$\begin{aligned} \mathrm{pAUC}_{\mathrm{Se}}(u \mid X) &= \int_u^1 \mathrm{ROC}_{\mathrm{Sp}}(p \mid X)\, \mathrm{d}p \\ &= [p\mathrm{ROC}_{\mathrm{Sp}}(p \mid X)]_u^1 - \int_u^1 p\, \mathrm{dROC}_{\mathrm{Sp}}(p \mid X) \\ &= -u\mathrm{ROC}_{\mathrm{Sp}}(u \mid X) - \int_u^1 p\, \mathrm{dROC}_{\mathrm{Sp}}(p \mid X), \end{aligned}$$

since $\mathrm{ROC}_{\mathrm{Sp}}(1 \mid X) = 0$ by definition; second, we have that

$$\begin{aligned}
-\mathrm{E}[\max\{u, Z_X\} \mid X] &= -\int_0^1 \max\{p, u\} \, \mathrm{d}F_{Z_X}(p \mid X) \\
&= \int_0^1 \max\{p, u\} \, \mathrm{d}S_{Z_X}(p \mid X) \\
&= \int_0^1 \max\{p, u\} \, \mathrm{dROC}_{\mathrm{Sp}}(p \mid X) \\
&= \int_0^1 pI(p > u) \, \mathrm{dROC}_{\mathrm{Sp}}(p \mid X) + \int_0^1 uI(u > p) \, \mathrm{dROC}_{\mathrm{Sp}}(p \mid X) \\
&= \int_u^1 p \, \mathrm{dROC}_{\mathrm{Sp}}(p \mid X) + u \int_0^u \mathrm{dROC}_{\mathrm{Sp}}(p \mid X) \\
&= \int_u^1 p \, \mathrm{dROC}_{\mathrm{Sp}}(p \mid X) + u\mathrm{ROC}_{\mathrm{Sp}}(u \mid X) - u.
\end{aligned}$$

Consequently,

$$\mathrm{E}[\max\{u, Z_X\} \mid X] - u = -\int_u^1 p \, \mathrm{dROC}_{\mathrm{Sp}}(p \mid X) - u\mathrm{ROC}_{\mathrm{Sp}}(u \mid X),$$

and thus, $\mathrm{pAUC}_{\mathrm{Se}}(u \mid X) = \mathrm{E}[\max\{u, Z_X\} \mid X] - u$, so that (1.1) holds.

1.2. *Calculus-based construction of our estimator.* We show that our estimator for $\mathrm{pAUC}_{\mathrm{TP}}$ can also be constructed by integrating our estimator of the $\mathrm{ROC}_{\mathrm{Sp}}$ curve, thus providing us with an alternative to the construction based on (1.1). Specifically, below we show that,

(1.2)
$$\widehat{\mathrm{pAUC}}_{\mathrm{Se}}(u \mid X) = \int_u^1 \widehat{\mathrm{ROC}}_{\mathrm{Sp}}(p \mid X)\mathrm{d}p = \frac{1}{n_{\bar{D}}} \sum_{i=1}^{n_{\bar{D}}} \max\left\{u, \frac{1}{n_D} \sum_{j=1}^{n_D} I(\widehat{Y}_{Dj|X} \geqslant Y_{\bar{D}i|X})\right\} - u,$$

where

$$\widehat{\mathrm{ROC}}_{\mathrm{Sp}}(p \mid X) = \widehat{F}_{\varepsilon_{\bar{D}}}\left\{\frac{\widehat{\mu}_D(X) - \widehat{\mu}_{\bar{D}}(X)}{\widehat{\sigma}_{\bar{D}}(X)} + \frac{\widehat{\sigma}_D(X)}{\widehat{\sigma}_{\bar{D}}(X)} \widehat{F}^{-1}_{\varepsilon_D}(1-p)\right\},$$

and where $\widehat{Y}_{\bar{D}i|X} = \widehat{\mu}_{\bar{D}}(X) + \widehat{\sigma}_{\bar{D}}(X)\widehat{\varepsilon}_{\bar{D}i}$, and $\widehat{Y}_{Dj|X} = \widehat{\mu}_D(X) + \widehat{\sigma}_D(X)\widehat{\varepsilon}_{Dj}$. Equation (1.2) follows by noting that

$$\begin{aligned}
\widehat{\mathrm{pAUC}}_{\mathrm{Se}}(u \mid X) &= \int_u^1 \widehat{\mathrm{ROC}}_{\mathrm{Sp}}(p \mid X) \, \mathrm{d}p \\
&= \int_u^1 \widehat{F}_{\varepsilon_{\bar{D}}}\left\{\frac{\widehat{\mu}_D(X) - \widehat{\mu}_{\bar{D}}(X)}{\widehat{\sigma}_{\bar{D}}(X)} + \frac{\widehat{\sigma}_D(X)}{\widehat{\sigma}_{\bar{D}}(X)} \widehat{F}^{-1}_{\varepsilon_D}(1-p)\right\} \mathrm{d}p \\
&= \int_u^1 \frac{1}{n_{\bar{D}}} \sum_{i=1}^{n_{\bar{D}}} I\left\{\widehat{\varepsilon}_{\bar{D}i} \leqslant \frac{\widehat{\mu}_D(X) - \widehat{\mu}_{\bar{D}}(X)}{\widehat{\sigma}_{\bar{D}}(X)} + \frac{\widehat{\sigma}_D(X)}{\widehat{\sigma}_{\bar{D}}(X)} \widehat{F}^{-1}_{\varepsilon_D}(1-p)\right\} \mathrm{d}p,
\end{aligned}$$

which implies that

$$\begin{aligned}\widehat{\mathrm{pAUC}}_{\mathrm{Se}}(u \mid X) &= \frac{1}{n_{\bar{D}}} \sum_{i=1}^{n_{\bar{D}}} \int_u^1 I\left\{p \leqslant 1 - \widehat{F}_{\varepsilon_D}\left(\frac{\widehat{\mu}_{\bar{D}}(X) - \widehat{\mu}_D(X)}{\widehat{\sigma}_D(X)} + \frac{\widehat{\sigma}_{\bar{D}}(X)}{\widehat{\sigma}_D(X)}\widehat{\varepsilon}_{\bar{D}i}\right)\right\} \mathrm{d}p \\ &= \frac{1}{n_{\bar{D}}} \sum_{i=1}^{n_{\bar{D}}} \int_u^{\max\left\{u, 1-\widehat{F}_{\varepsilon_D}\left(\frac{\widehat{\mu}_{\bar{D}}(X)-\widehat{\mu}_D(X)}{\widehat{\sigma}_D(X)} + \frac{\widehat{\sigma}_{\bar{D}}(X)}{\widehat{\sigma}_D(X)}\widehat{\varepsilon}_{\bar{D}i}\right)\right\}} \mathrm{d}p \\ &= \frac{1}{n_{\bar{D}}} \sum_{i=1}^{n_{\bar{D}}} \max\left\{u, \frac{1}{n_D}\sum_{j=1}^{n_D}(\widehat{Y}_{Dj|X} \geqslant \widehat{Y}_{\bar{D}i|X})\right\} - u.\end{aligned}$$

2. Supplementary exploratory analysis.

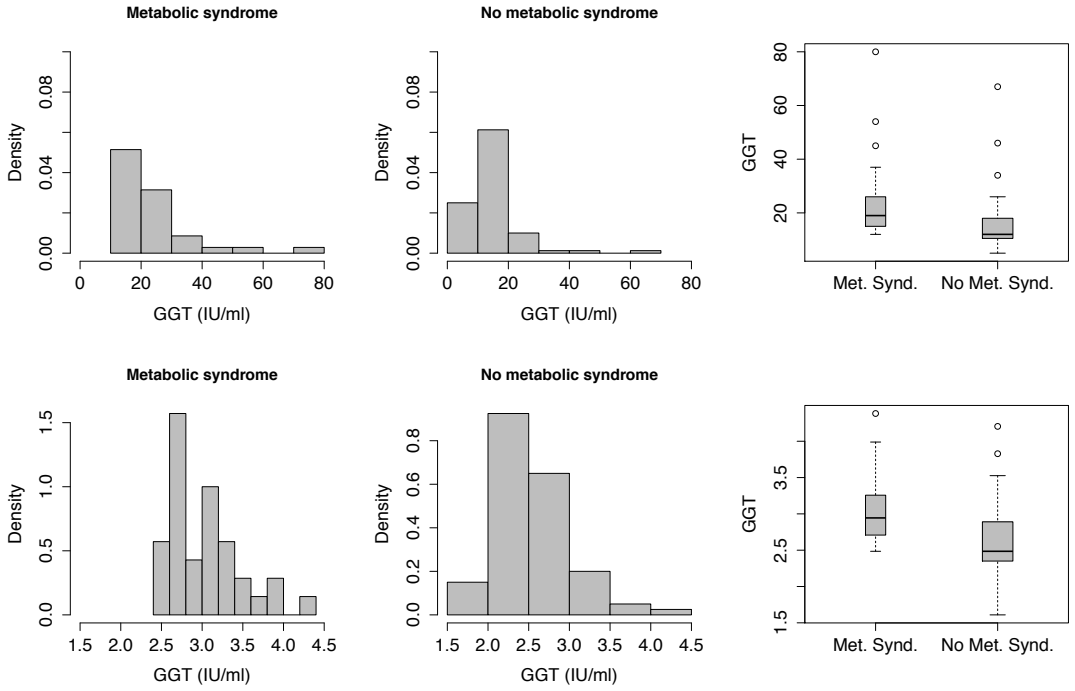

FIG 1. *Histogram and variable-width boxplot of GGT levels (for 35 women with and 80 without metabolic syndrome) in the original scale (top) and in the log scale (bottom).*

u	0	0.6	0.7	0.8	0.9	0.95
$\widehat{\text{Average}}\ \mathrm{Sp}(u)$	0.790	0.618	0.595	0.561	0.504	0.459
(95% bootstrap CI)	(0.709, 0.868)	(0.512, 0.734)	(0.468, 0.717)	(0.437, 0.689)	(0.375, 0.645)	(0.330, 0.630)

TABLE 1

Estimated average specificity and its corresponding 95% bootstrap confidence interval for the no arterial oxygen saturation-adjusted analysis.

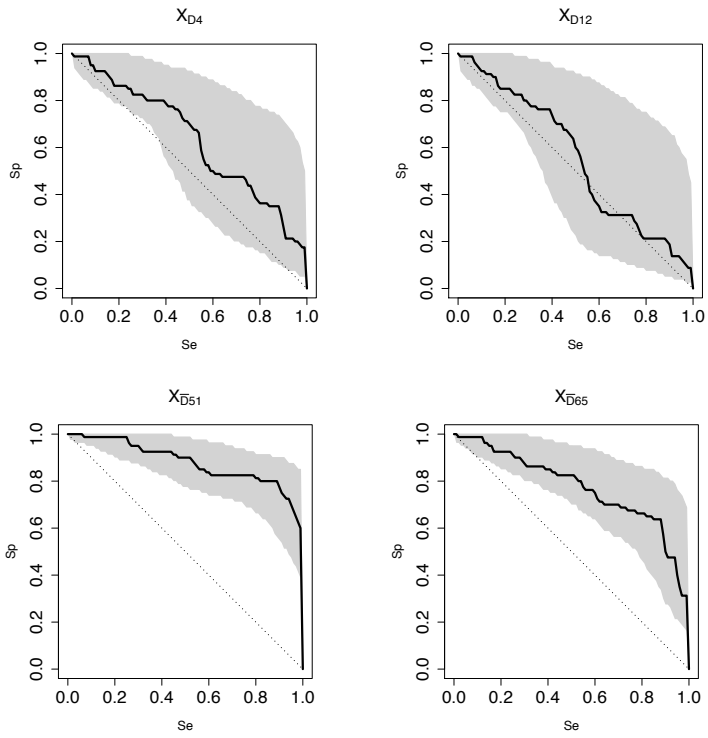

FIG 2. *ROC_{Sp} curves corresponding to the four curves of arterial oxygen saturation displayed in Figure 4 of the main manuscript.*

We assess the ability of the arterial oxygen saturation curves themselves for discriminating between women with and without metabolic syndrome. To this end, we carried out a functional principal component analysis of the arterial oxygen saturation curves by pooling together the 115 curves. The estimated functional principal component scores, presented in Figure 3 (a), that are often viewed as subject-specific summaries (Yao, Fu, and Lee, 2011), show a separation between women with metabolic syndrome and women without metabolic syndrome, reinforcing that the arterial oxygen curves have a different pattern in the two groups. These first two components account for 83% of the variation in the data (76% (7%) the first (second) principal component). To further examine the discriminatory ability of the oxygen saturation curves, we have estimated the nonparametric kernel-based ROC curve proposed by Lloyd (1998) associated with the estimated first principal component scores, where the bandwidths were selected using the Hall–Hyndman method (Hall and Hyndman, 2003); see Figure 3 (c). The estimated AUC is 0.811 $(0.727, 0.887)$, revealing a good separation of the estimated first scores in the two groups of women.

3. Comparison with approaches based on an univariate covariate. For the metabolic syndrome data, we have compared our approach with two simpler approaches: one based on the mean oxygen saturation and another based on the minimum oxygen saturation. We have thus compared our estimator which relies on functional nonparametric regression with two estimators that are based on univariate kernel regression (González-Manteiga, Pardo-Fernández, and Van Keilegom, 2011). Table 2 presents the estimated average specificity, over the different intervals of sensitivity considered in Section 4 of the main manuscript, for the curves presented

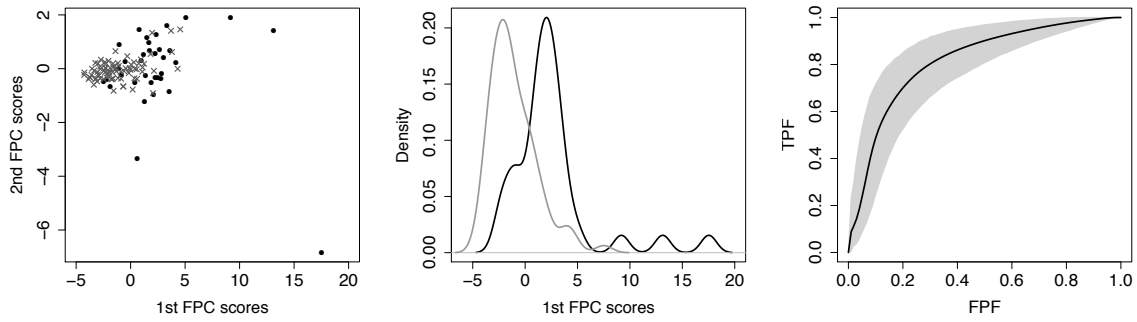

(a) (b) (c)

FIG 3. *(a) First and second estimated functional principal component scores of the oxygen saturation curves for women with metabolic syndrome (•) and for women without metabolic syndrome (×). (b) Kernel density estimate of the 1st scores for women without metabolic syndrome (gray) and for women with metabolic syndrome (black). (c) Kernel-based ROC curve associated with the estimated scores of the first functional principal component. Estimate (black) and* 95% *bootstrap confidence bands (gray).*

in Figure 4 (a). As can be observed, there is a clear difference between our functional approach and the two simpler approaches based on univariate summary measures of the oxygen saturation curves. Of course, we do recognize that the confidence intervals are in some cases wide. We have also conducted a similar analysis but with simulated data. Specifically, for the data simulated in Section 5, under Scenario 1, and for the sample size (n_0, n_1), we have estimated the average specificity for the 400 generated curves. For the curves presented in Figure 4 (b), Table 3 summarizes the results obtained under the three distinct approaches considered versus the average specificity values. The results are based on 1000 repetitions. Specifically, what it is presented is the mean of the estimated average specificity across the 1000 simulated data sets along with the 2.5% and 97.5% simulation quantiles (in brackets). As can be observed, for the three chosen curves, the functional approach presents a better behavior. We end remarking that we are not claiming that the results between an approach using a functional covariate and an approach based on an univariate summary covariate are always different, we are only providing evidence that they do not have always to coincide.

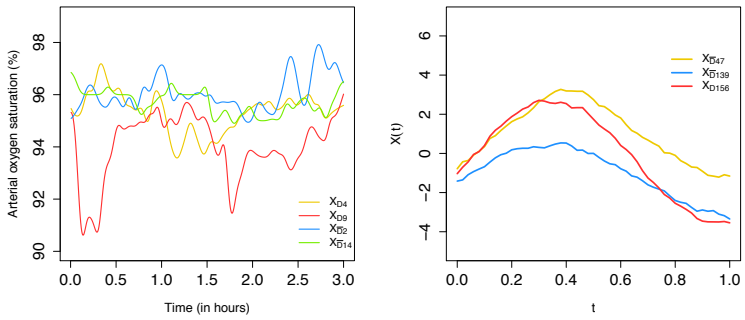

(a) (b)

FIG 4. *(a) Arterial oxygen saturation curves* X_{D4}, X_{D9}, $X_{\bar{D}2}$, *and* $X_{\bar{D}14}$. *(b) Simulated curves* $X_{\bar{D}47}$, $X_{\bar{D}139}$, *and* $X_{\bar{D}14}$.

	Average specificity		
X_{D4}	Functional covariate	Mean	Minimum
$u = 0$	0.631 (0.493, 0.863)	0.521 (0.385, 0.814)	0.701 (0.502, 0.901)
$u = 0.6$	0.357 (0.160, 0.735)	0.182 (0.067, 0.648)	0.456 (0.168, 0.811)
$u = 0.7$	0.317 (0.131, 0.702)	0.172 (0.047, 0.607)	0.401 (0.121, 0.785)
$u = 0.8$	0.263 (0.105, 0.659)	0.157 (0.034, 0.562)	0.343 (0.086, 0.763)
$u = 0.9$	0.191 (0.075, 0.600)	0.123 (0.014, 0.488)	0.230 (0.053, 0.722)
$u = 0.95$	0.173 (0.055, 0.561)	0.113 (0.011, 0.438)	0.143 (0.038, 0.686)
X_{D9}			
$u = 0$	0.511 (0.192, 0.885)	0.741 (0.454, 0.962)	0.766 (0.405, 0.969)
$u = 0.6$	0.163 (0.021, 0.789)	0.516 (0.142, 0.918)	0.563 (0.085, 0.930)
$u = 0.7$	0.148 (0.015, 0.753)	0.475 (0.117, 0.903)	0.509 (0.052, 0.910)
$u = 0.8$	0.123 (0.009, 0.707)	0.409 (0.093, 0.888)	0.455 (0.030, 0.890)
$u = 0.9$	0.080 (0.000, 0.620)	0.266 (0.060, 0.858)	0.338 (0.005, 0.851)
$u = 0.95$	0.075 (0.000, 0.543)	0.213 (0.038, 0.831)	0.223 (0.000, 0.807)
$X_{\bar{D}2}$			
$u = 0$	0.672 (0.764, 0.912)	0.546 (0.796, 0.894)	0.821 (0.699, 0.950)
$u = 0.6$	0.579 (0.407, 0.826)	0.454 (0.215, 0.786)	0.662 (0.454, 0.911)
$u = 0.7$	0.542 (0.351, 0.800)	0.404 (0.178, 0.761)	0.621 (0.400, 0.897)
$u = 0.8$	0.479 (0.260, 0.777)	0.345 (0.144, 0.734)	0.570 (0.321, 0.886)
$u = 0.9$	0.366 (0.180, 0.729)	0.216 (0.106, 0.701)	0.482 (0.230, 0.870)
$u = 0.95$	0.305 (0.146, 0.704)	0.200 (0.080, 0.677)	0.391 (0.154, 0.854)
$X_{\bar{D}14}$			
$u = 0$	0.696 (0.593, 0.887)	0.600 (0.472, 0.852)	0.818 (0.696, 0.951)
$u = 0.6$	0.455 (0.297, 0.778)	0.270 (0.122, 0.713)	0.655 (0.460, 0.912)
$u = 0.7$	0.413 (0.248, 0.751)	0.232 (0.098, 0.673)	0.615 (0.388, 0.896)
$u = 0.8$	0.354 (0.187, 0.707)	0.204 (0.080, 0.659)	0.563 (0.314, 0.882)
$u = 0.9$	0.248 (0.123, 0.668)	0.148 (0.050, 0.613)	0.470 (0.223, 0.859)
$u = 0.95$	0.200 (0.100, 0.630)	0.138 (0.038, 0.586)	0.373 (0.153, 0.838)

TABLE 2

Estimated average specificity for arterial oxygen saturation curves X_{D4}, X_{D9}, $X_{\bar{D}2}$, and $X_{\bar{D}14}$ along with 95% bootstrap confidence intervals.

	Average specificity		
$X_{\bar{D}47}$	Functional covariate	Mean	Minimum
$u = 0$			
(**0.886**)	0.872 (0.728, 0.965)	0.794 (0.702, 0.870)	0.707 (0.614, 0.797)
$u = 0.6$			
(**0.716**)	0.690 (0.367, 0.913)	0.515 (0.328, 0.685)	0.384 (0.241, 0.544)
$u = 0.8$			
(**0.495**)	0.479 (0.122, 0.828)	0.275 (0.109, 0.477)	0.184 (0.068, 0.342)
$u = 0.95$			
(**0.117**)	0.153 (0.004, 0.525)	0.051 (0.003, 0.168)	0.025 (0.000, 0.099)
$X_{\bar{D}139}$			
$u = 0$			
(**0.724**)	0.724 (0.486, 0.883)	0.638 (0.500, 0.763)	0.555 (0.363, 0.729)
$u = 0.6$			
(**0.367**)	0.388 (0.075, 0.709)	0.249 (0.089, 0.456)	0.180 (0.029, 0.429)
$u = 0.8$			
(**0.133**)	0.172 (0.009, 0.493)	0.082 (0.009, 0.217)	0.056 (0.001, 0.222)
$u = 0.95$			
(**0.007**)	0.023 (0.000, 0.139)	0.007 (0.000, 0.039)	0.006 (0.000, 0.049)
X_{D156}			
$u = 0$			
(**0.845**)	0.811 (0.548, 0.973)	0.720 (0.613, 0.812)	0.545 (0.353, 0.731)
$u = 0.6$			
(**0.621**)	0.566 (0.120, 0.933)	0.373 (0.207, 0.553)	0.171 (0.021, 0.434)
$u = 0.8$			
(**0.368**)	0.357 (0.016, 0.870)	0.157 (0.044, 0.317)	0.054 (0.000, 0.226)
$u = 0.95$			
(**0.059**)	0.113 (0.000, 0.595)	0.019 (0.000, 0.083)	0.007 (0.000, 0.050)

TABLE 3

Estimated mean average specificity for simulated curves $X_{\bar{D}47}$, $X_{\bar{D}139}$, and X_{D156} across the 1000 simulated along with the 2.5% and 97.5% simulation quantiles. In bold we present the true average specificity.

4. Supplementary reports on numerical experiments.

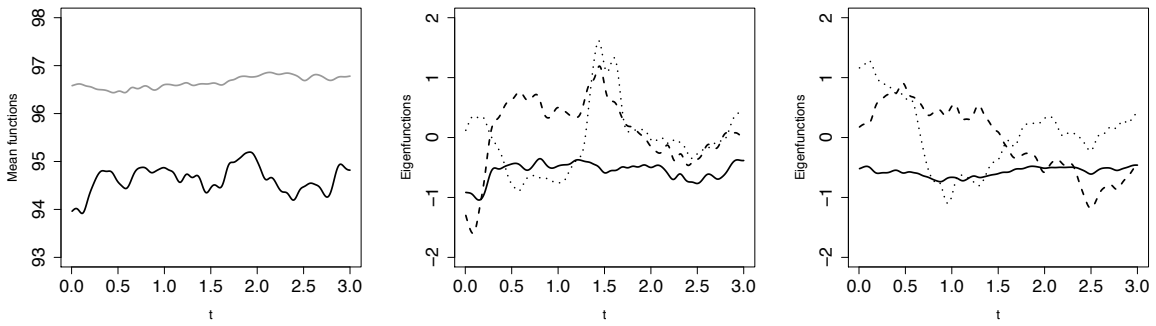

(a) (b) (c)

FIG 5. *(a) Mean functions, obtained from the metabolic syndrome study data, for diseased (black) and non-diseased (gray) groups. (b) Estimated first (solid line), second (dashed line), and third (dotted line) eigenfunctions from the metabolic syndrome data for the diseased group. (c) Estimated first (solid line), second (dashed line), and third (dotted line) eigenfunctions from the metabolic syndrome data for the non diseased group.*

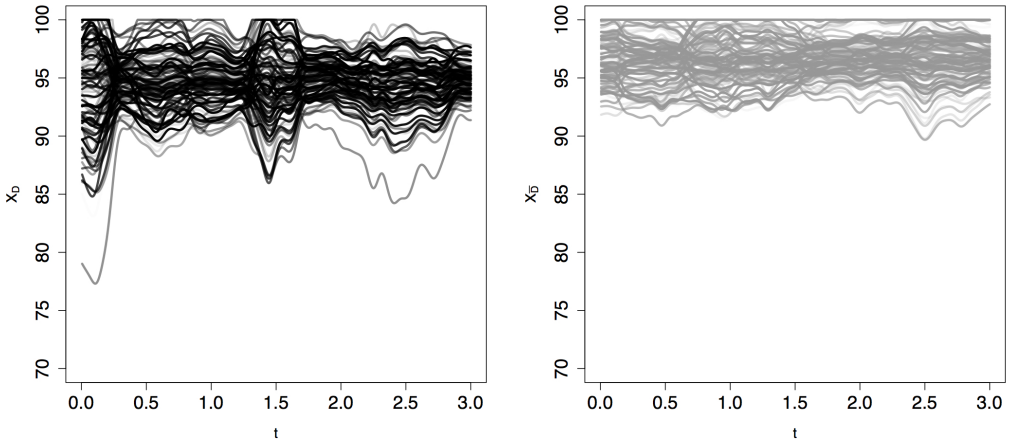

(a) (b)

FIG 6. *Covariate curves generated according to Eq. (5.1) in the article, from one simulation run, mimicking those from the metabolic syndrome case study. (a) Diseased group. (b) Non-Diseased group.*

Results for Scenario A

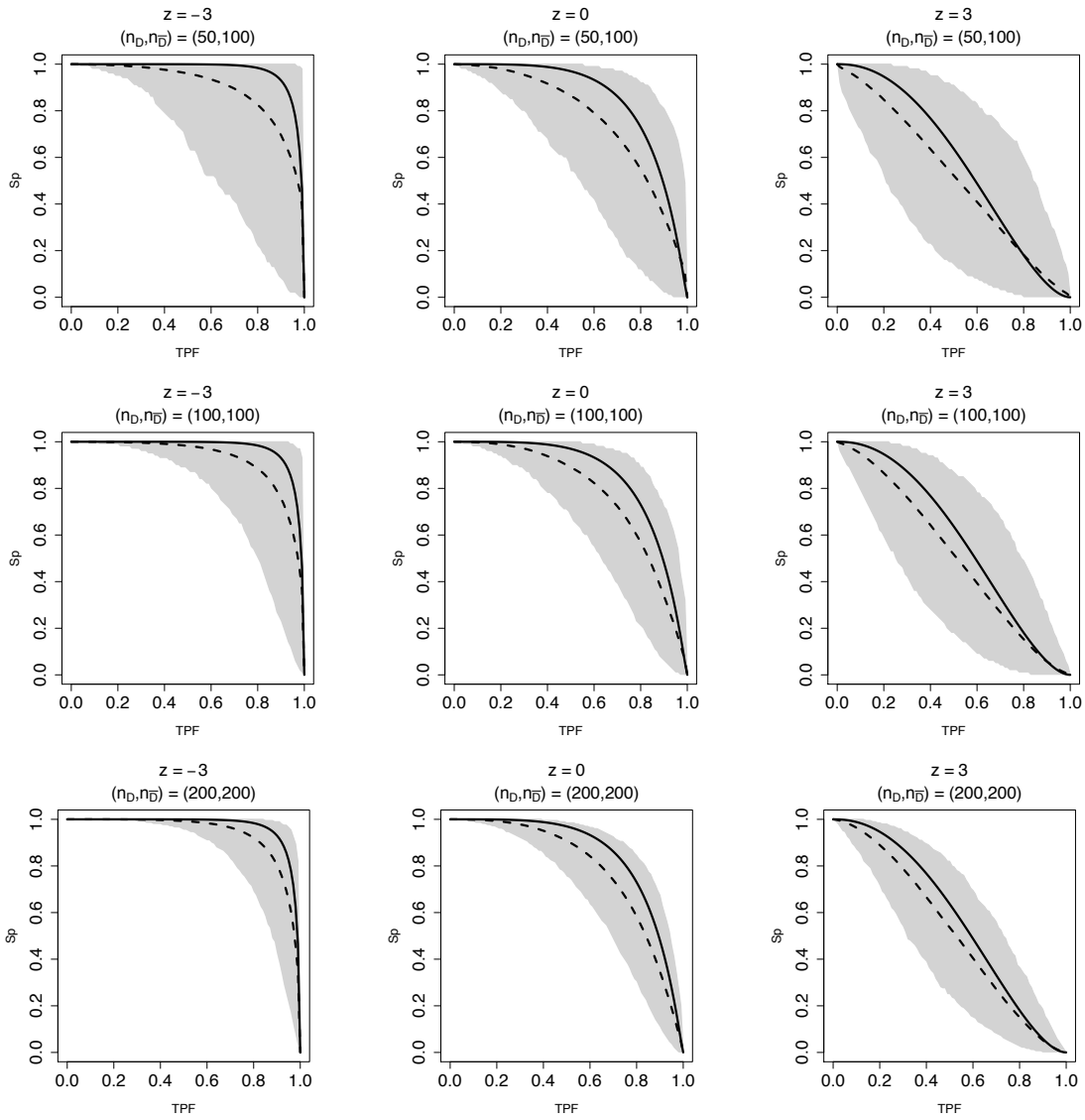

FIG 7. *Results for Scenario A. True ROC_{Sp} curve (solid line) versus the mean of Monte Carlo estimates (dashed line) along with* 2.5% *and* 97.5% *simulation quantiles (gray area) for* $z = -3, 0,$ *and* 3.

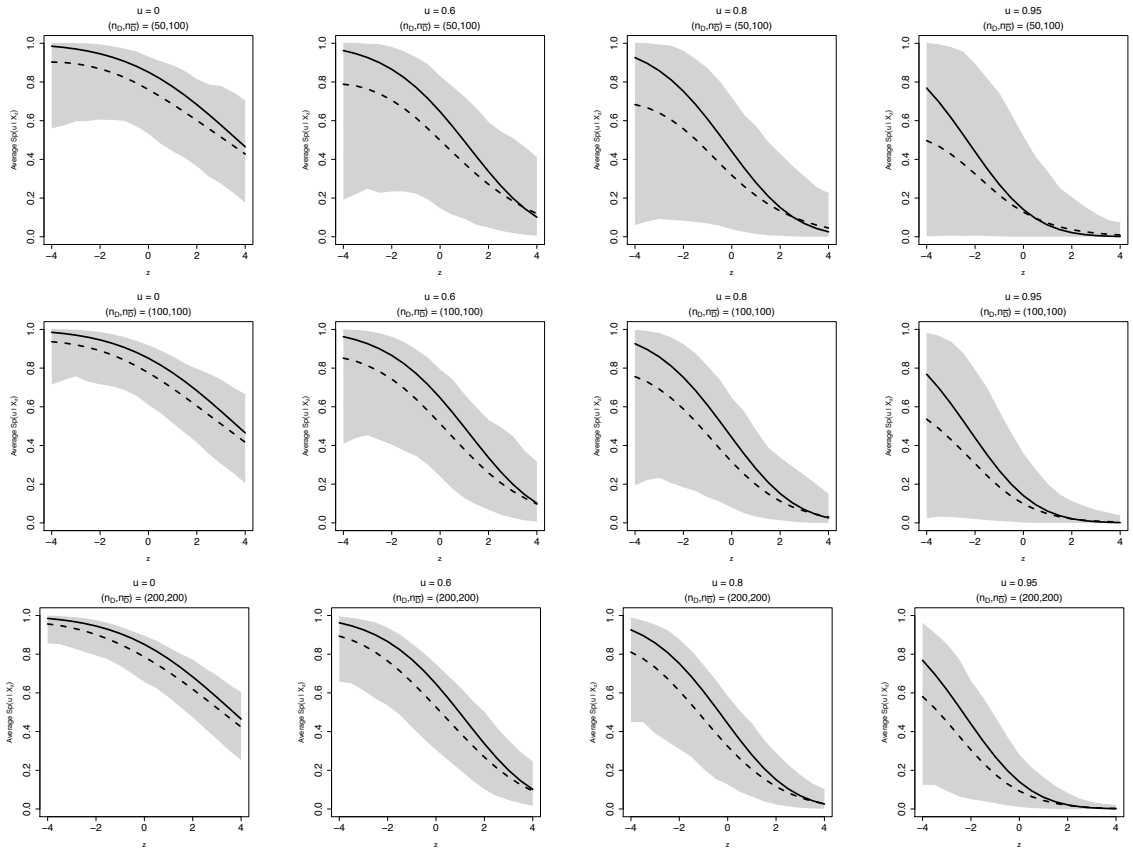

FIG 8. *Results for Scenario A. True functional covariate-adjusted average specificity (solid line) versus the mean of Monte Carlo estimates (dashed line) along with* 2.5% *and* 97.5% *simulation quantiles (gray area) for* $u = 0, 0.6, 0.8,$ *and* 0.95.

Results for Scenario B

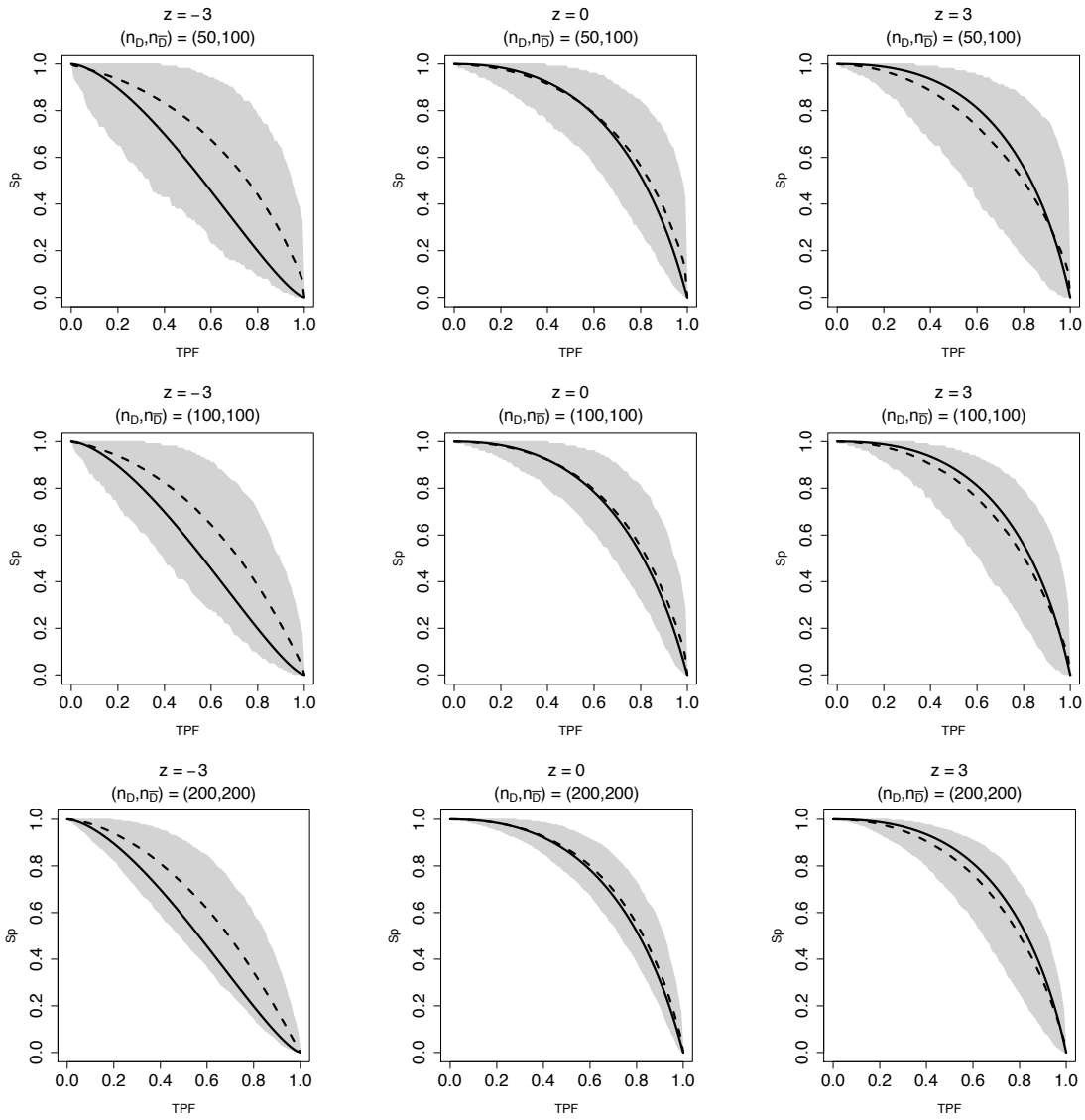

FIG 9. *Results for Scenario B. True ROC_{Sp} curve (solid line) versus the mean of Monte Carlo estimates (dashed line) along with* 2.5% *and* 97.5% *simulation quantiles (gray area) for* $z = -3, 0,$ *and* 3.

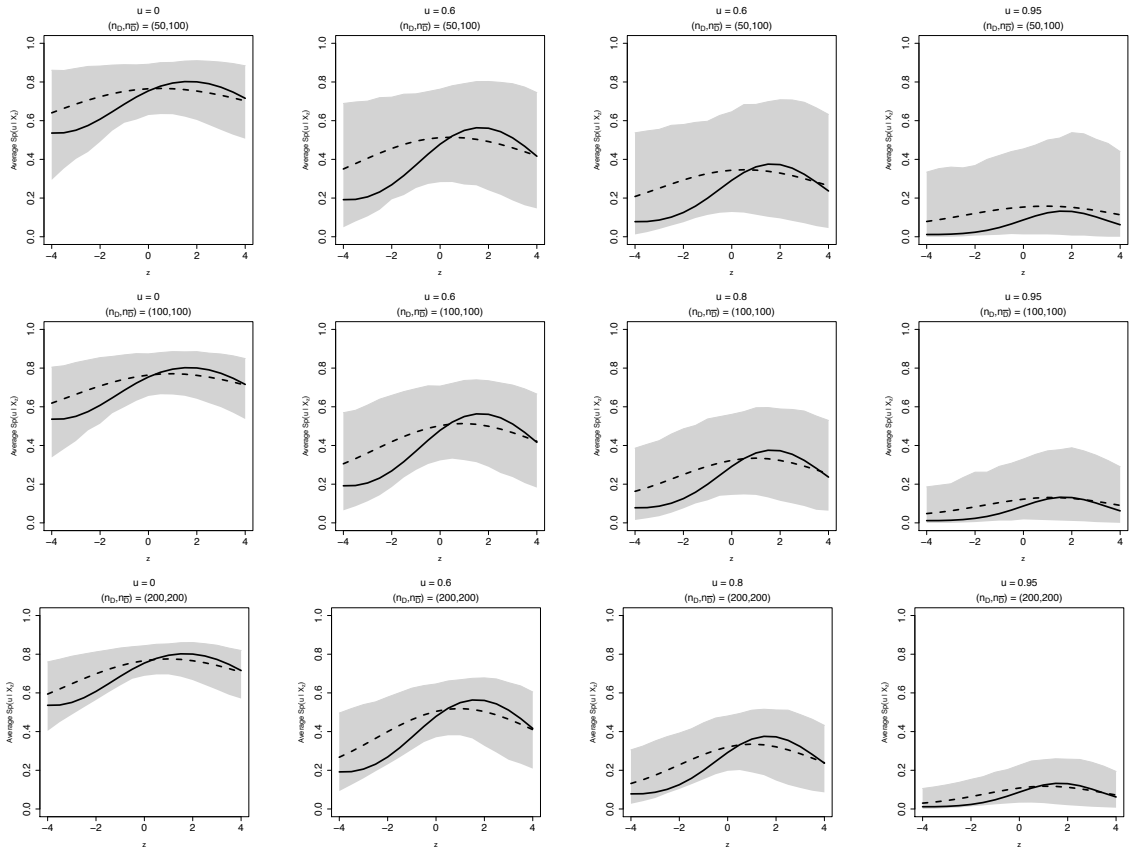

FIG 10. *Results for Scenario B. True functional covariate-adjusted average specificity (solid line) versus the mean of Monte Carlo estimates (dashed line) along with* 2.5% *and* 97.5% *simulation quantiles (gray area) for* $u = 0, 0.6, 0.8,$ *and* 0.95.

5. Additional simulation study. We describe and report an additional simulation study whose main aim is to ascertain the performance of the proposed estimator in a general setup. Here, the covariate trajectories for the diseased and non-diseased groups were evaluated discretely on an equally spaced grid of 51 points of $[0,1]$, generated with a trend function $X_0(t) = t + \sin(t)$ and a covariance function derived from two eigenfunctions: $v_1(t) = \sqrt{2}\sin(0.5\pi t)$ and $v_2(t) = \sqrt{2}\sin(1.5\pi t)$, associated with the eigenvalues $\lambda_1 = 4$ and $\lambda_2 = 1$; the covariate functional principal component scores are $\gamma_l \sim \mathrm{N}(0, \lambda_l)$, $l = 1, 2$. In short, the covariate trajectories for each group were, independently, generated using the following representation

$$X_D(t) = X_0(t) + \sum_{l=1}^{2} \gamma_l v_l(t), \quad X_{\bar{D}}(t) = X_0(t) + \sum_{l=1}^{2} \gamma_l v_l(t), \quad 0 \leqslant t \leqslant 1. \tag{5.1}$$

To fix ideas, Figure 11 (a) presents a sample of 50 such curves.

We consider four data-generating configurations (Scenarios 1, 2, 3, and 4) and, for each scenario, 1000 datasets were generated for each of three different sample sizes: $(n_D, n_{\bar{D}}) = (50, 100)$, $(n_D, n_{\bar{D}}) = (100, 100)$, and $(n_D, n_{\bar{D}}) = (200, 200)$. Specifically, in the four generated scenarios, we assume the following regression models for the marker outcome in the diseased and non-diseased groups

$$\begin{cases} Y_{\bar{D}} = 1.5 + \langle \beta, X_{\bar{D}} \rangle + \varepsilon_{\bar{D}}, \quad Y_D = 3 + 1.5\langle \beta, X_D \rangle + 2\varepsilon_D, & \text{(Scenario 1)} \\ Y_{\bar{D}} = \langle \beta, \sin(X_{\bar{D}} + 0.5) \rangle + 1.5\varepsilon_{\bar{D}}, \quad Y_D = 1.5 + 0.5\langle \beta, \sin(X_D + 0.25) \rangle + 2\varepsilon_D, & \text{(Scenario 2)} \\ Y_{\bar{D}} = \langle \beta, X_{\bar{D}}^2 \rangle + \{\langle \beta, \exp(X_{\bar{D}}) \rangle\}^{1/2}\varepsilon_{\bar{D}}, \quad Y_D = 1.5 + \langle \beta, (X_D + 0.5)^2 \rangle + 2\varepsilon_D, & \text{(Scenario 3)} \\ Y_{\bar{D}} = (1 + |\langle \beta, X_{\bar{D}} \rangle|)^{\varepsilon_{\bar{D}}}, \quad Y_D = (2 + |\langle \beta, X_D \rangle|)^{\varepsilon_D}. & \text{(Scenario 4)} \end{cases}$$

In all scenarios, $\langle \beta, X_s \rangle = \int_0^1 \beta(t) X_s(t) \mathrm{d}t$, for $s \in \{D, \bar{D}\}$, $\beta(t) = v_1(t) + v_2(t)$, and X_D and $X_{\bar{D}}$ were independently generated using (5.1). In Scenario 1, 2, and 3, ε_D and $\varepsilon_{\bar{D}}$ follow the standard normal distribution, while in Scenario 4, $\varepsilon_{\bar{D}}$ follows the standard normal distribution, but $\varepsilon_D \sim \mathrm{SN}(0, 1, \langle \beta, X_D \rangle)$, where $\mathrm{SN}(\mu, \sigma, \alpha)$ denotes the skew normal distribution with mean μ, standard deviation σ, and shape α. Note that in Scenario 4 we are simultaneously violating the two assumptions underlying our model; specifically, the model for the marker outcomes of both groups does not belong to a location-scale family and the error in the diseased group depends on the covariate X (through the shape parameter). The purpose of including Scenario 4 is to evaluate the performance of our estimator when the assumptions underlying its construction do not hold. Under the above configurations, the true average specificity for Scenarios 1, 2, 3, and 4 are, respectively

$$\text{Average } \mathrm{Sp}(u \mid X) = \begin{cases} \int_u^1 \Phi\left(1.5 + 0.5\langle \beta, X \rangle + 2\Phi^{-1}(1-p)\right) \mathrm{d}p/(1-u), \\ \int_u^1 \Phi\left(\frac{1.5 + 0.5\langle \beta, \sin(X+0.25) \rangle - \langle \beta, \sin(X+0.5) \rangle}{1.5} + \frac{2}{1.5}\Phi^{-1}(1-p)\right) \mathrm{d}p/(1-u), \\ \int_u^1 \Phi\left(\frac{1.5 + \langle \beta, (X+0.5)^2 \rangle - \langle \beta, X^2 \rangle}{\{\langle \beta, \exp(X) \rangle\}^{1/2}} + \frac{2}{\{\langle \beta, \exp(X) \rangle\}^{1/2}}\Phi^{-1}(1-p)\right) \mathrm{d}p/(1-u), \\ \int_u^1 \Phi\left(\frac{\log(2 + \langle \beta, X \rangle)\Phi_{\mathrm{SN}}(1-p, 0, 1, \langle \beta, X \rangle)}{\log(1 + \langle \beta, X \rangle)}\right) \mathrm{d}p/(1-u), \end{cases}$$

where numerical integration is used to evaluate each integral. We consider four different values of u: $0, 0.6, 0.8$, and 0.95, and we consider the following 'grid' of curves conditionally on which we predict the average specificity, i.e.,

$$X_z(t) = X_0(t) + z v_1(t), \quad t \in [0,1], \quad z \in \mathcal{Z} = \{-2\sqrt{\lambda_1} + k : k \in \{0, 1, \ldots, 4\sqrt{\lambda_1}\}\}. \tag{5.2}$$

This grid of curves resembles the range of variation of curves simulated through (5.1) and we set z to be in the range of the first principal component scores γ_1; thus, since $\gamma_1 \sim \mathrm{N}(0, \lambda_1)$, we set z to vary between $(-2\sqrt{\lambda_1}, 2\sqrt{\lambda_1})$. Figure 11 (b) depicts the shape of the grid of curves defined by (5.2), and Figure 11 (c) shows the curves corresponding to z values of -2, 0, and 3.

5.1. *Simulation results.* Our estimator was implemented using the asymmetric Gaussian Kernel, the bandwidths were selected using generalized cross validation, and the semimetric d is the $L^2[0,1]$-norm.

Scenarios 1–3: Figures 12, 14, and 16 show the true $\mathrm{ROC}_{\mathrm{Sp}}$ curves, for Scenarios 1, 2, and 3, respectively, along with the estimated Monte Carlo averages and the 2.5% and 97.5% simulation quantiles corresponding to the covariate curves associated with z values equal to -2, 0, and 3 (and which are depicted on Figure 11 (c)). From these figures it can be observed that our estimator is able to successfully recover the true shape of the different $\mathrm{ROC}_{\mathrm{Sp}}$ curves. In turn, in Figures 13, 15, and 17, we present the true functional covariate-adjusted average specificity versus the Monte Carlo averages of the estimated functional covariate-adjusted average specificities, along with the 2.5% and 97.5% simulation quantiles. From these figures it can be concluded that our estimator is able to recover the true functional shape of the average specificity and that as the sample size increases and more of the curve is integrated out, the bias becomes negligible.

Scenario 4: Figure 18 shows the true $\mathrm{ROC}_{\mathrm{Sp}}$ curves, while Figure 19 shows the true functional covariate-adjusted average specificity. From these figures we can notice that the even when the assumptions underlying our estimator are violated, the estimator is still able to recover reasonably well the true average specificity curve, although with more bias and higher variance.

It is also worth to note that, as expected, as the complexity of the simulation scenario increases, the $2.5\% - 97.5\%$ simulation bands get wider (with exception of Scenario 2, for which we do not see any obvious reason).

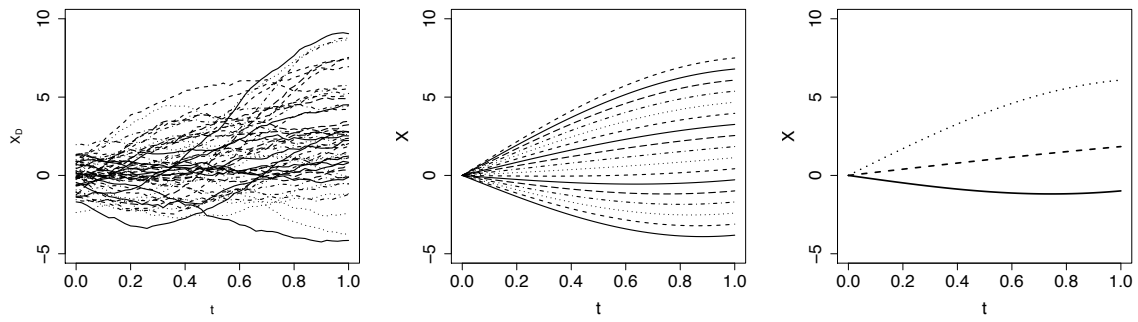

(a) (b) (c)

FIG 11. *(a) Simulated covariate curves, X_D; a similar representation holds for $X_{\bar{D}}$. (b) Curves generated according to (5.1) in the article and conditionally on which we predict the average specificity. (c) Curves corresponding to $z = -2$ (solid line), $z = 0$ (dashed line), and $z = 3$ (dotted line).*

Results for Scenario 1

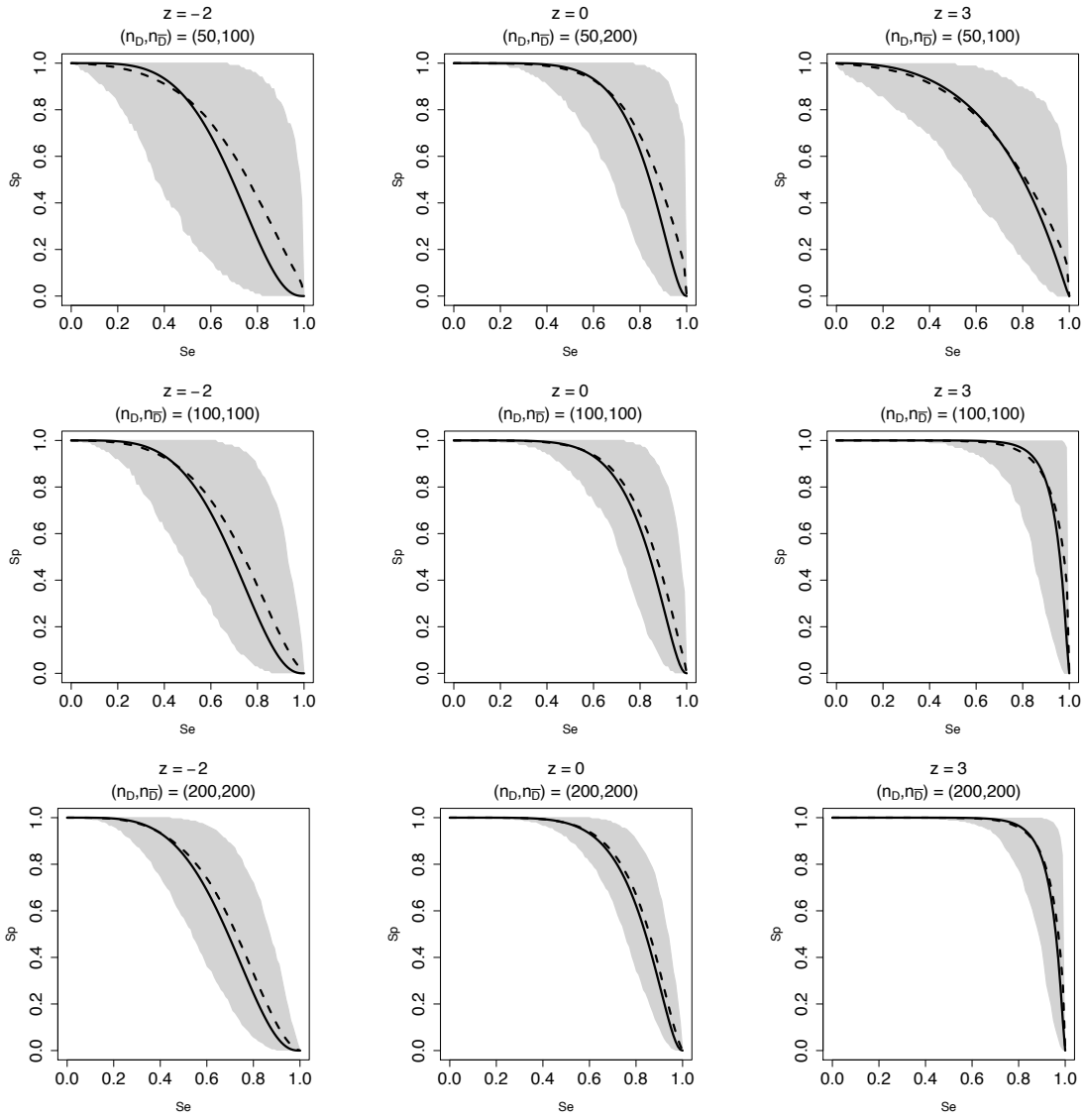

FIG 12. *Results for Scenario 1. True ROC_{Sp} curve (solid line) versus the mean of Monte Carlo estimates (dashed line) along with* 2.5% *and* 97.5% *simulation quantiles (gray area) for* $z = -2, 0,$ *and* 3.

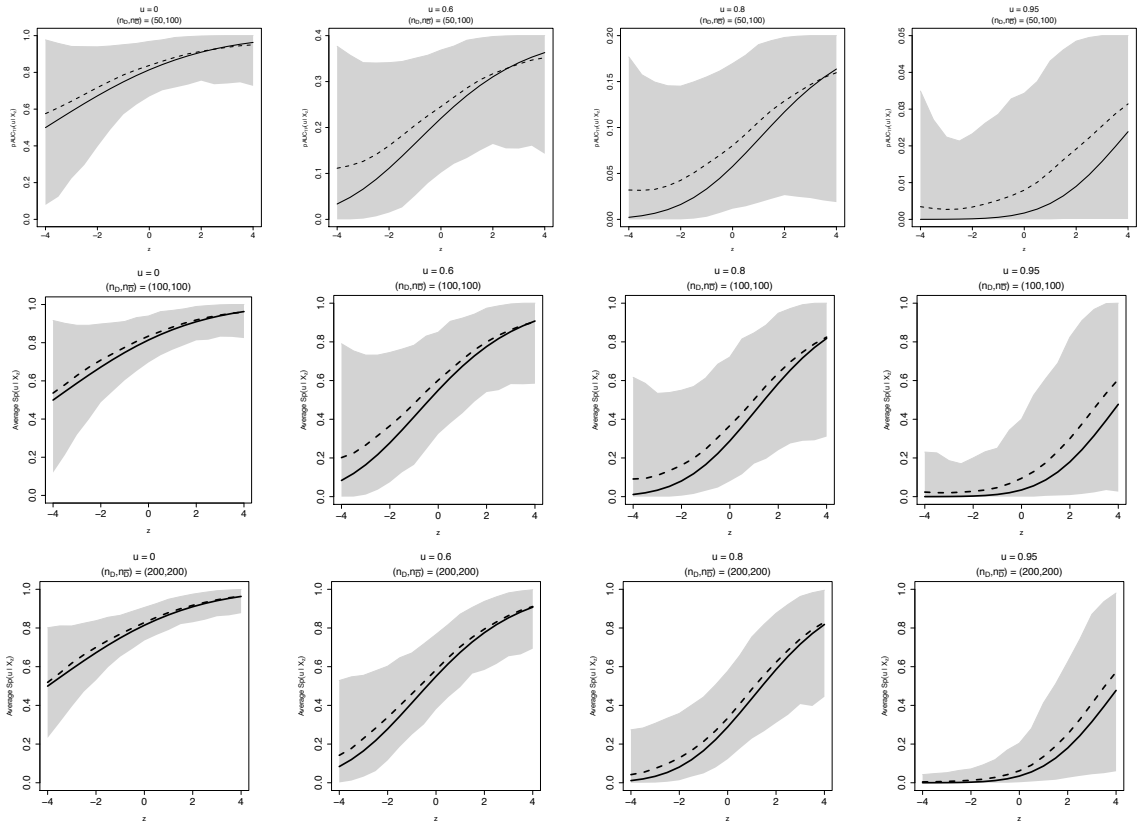

FIG 13. *Results for Scenario 1. True functional covariate-adjusted average specificity (solid line) versus the mean of Monte Carlo estimates (dashed line) along with* 2.5% *and* 97.5% *simulation quantiles (gray area) for* $u = 0, 0.6, 0.8,$ *and* 0.95.

Results for Scenario 2

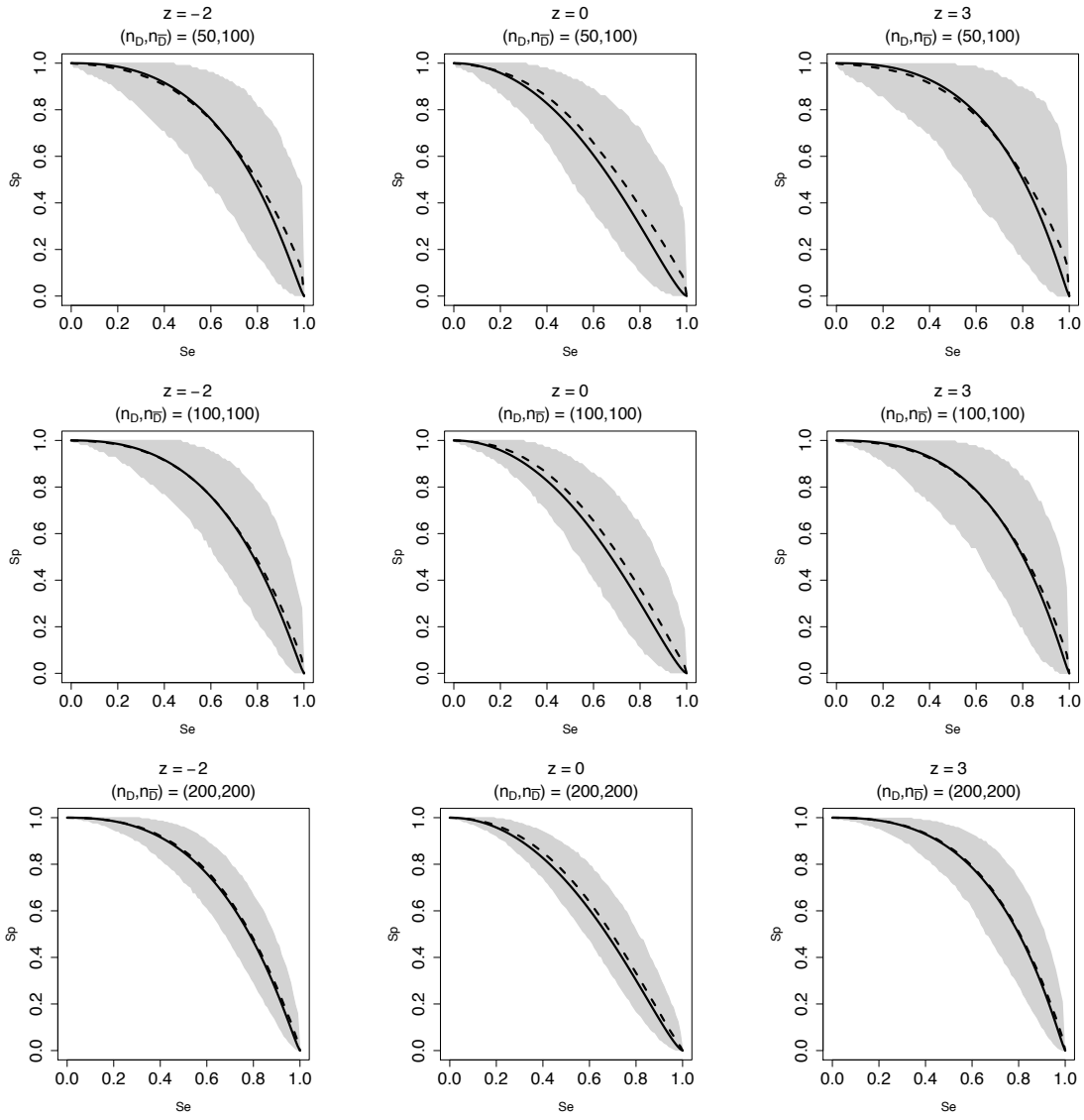

FIG 14. *Results for Scenario 2. True ROC_{Sp} curve (solid line) versus the mean of Monte Carlo estimates (dashed line) along with* 2.5% *and* 97.5% *simulation quantiles (gray area) for* $z = -2, 0,$ *and* 3.

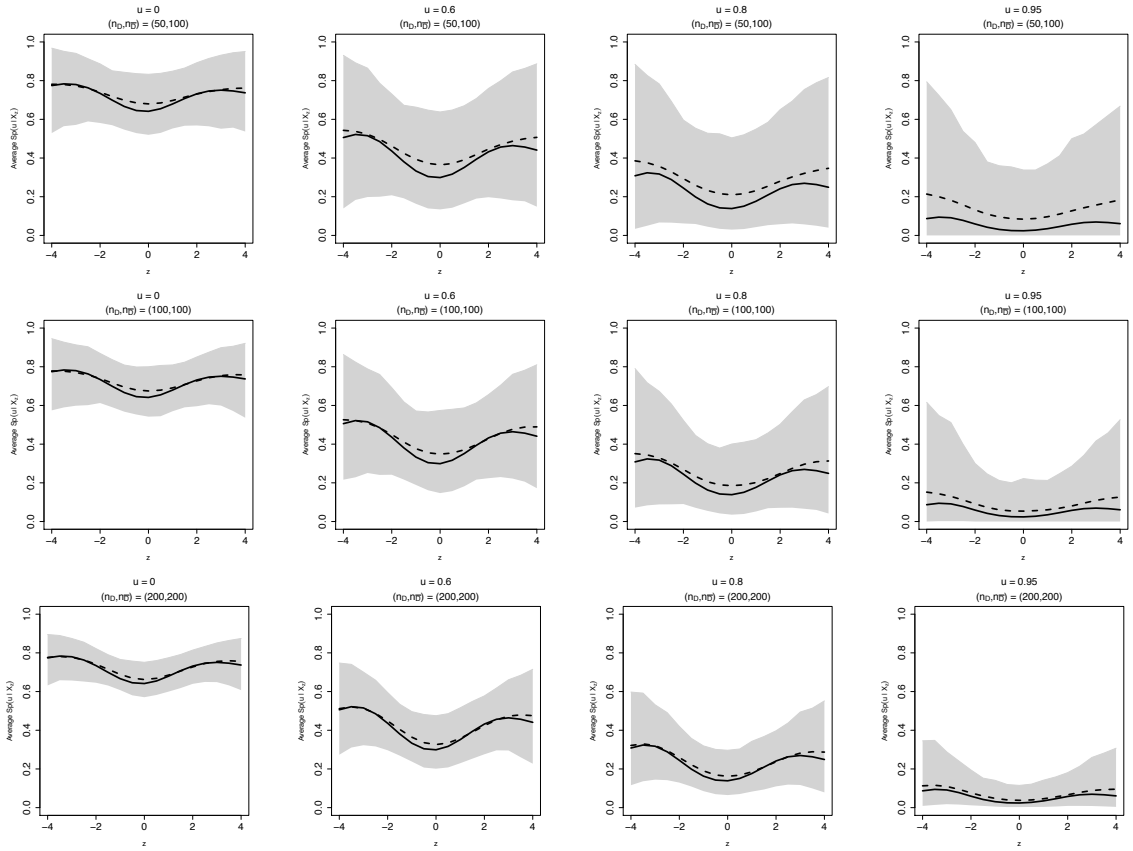

FIG 15. *Results for Scenario 2. True functional covariate-adjusted average specificity (solid line) versus the mean of Monte Carlo estimates (dashed line) along with* 2.5% *and* 97.5% *simulation quantiles (gray area) for* $u = 0, 0.6, 0.8,$ *and* 0.95.

Results for Scenario 3

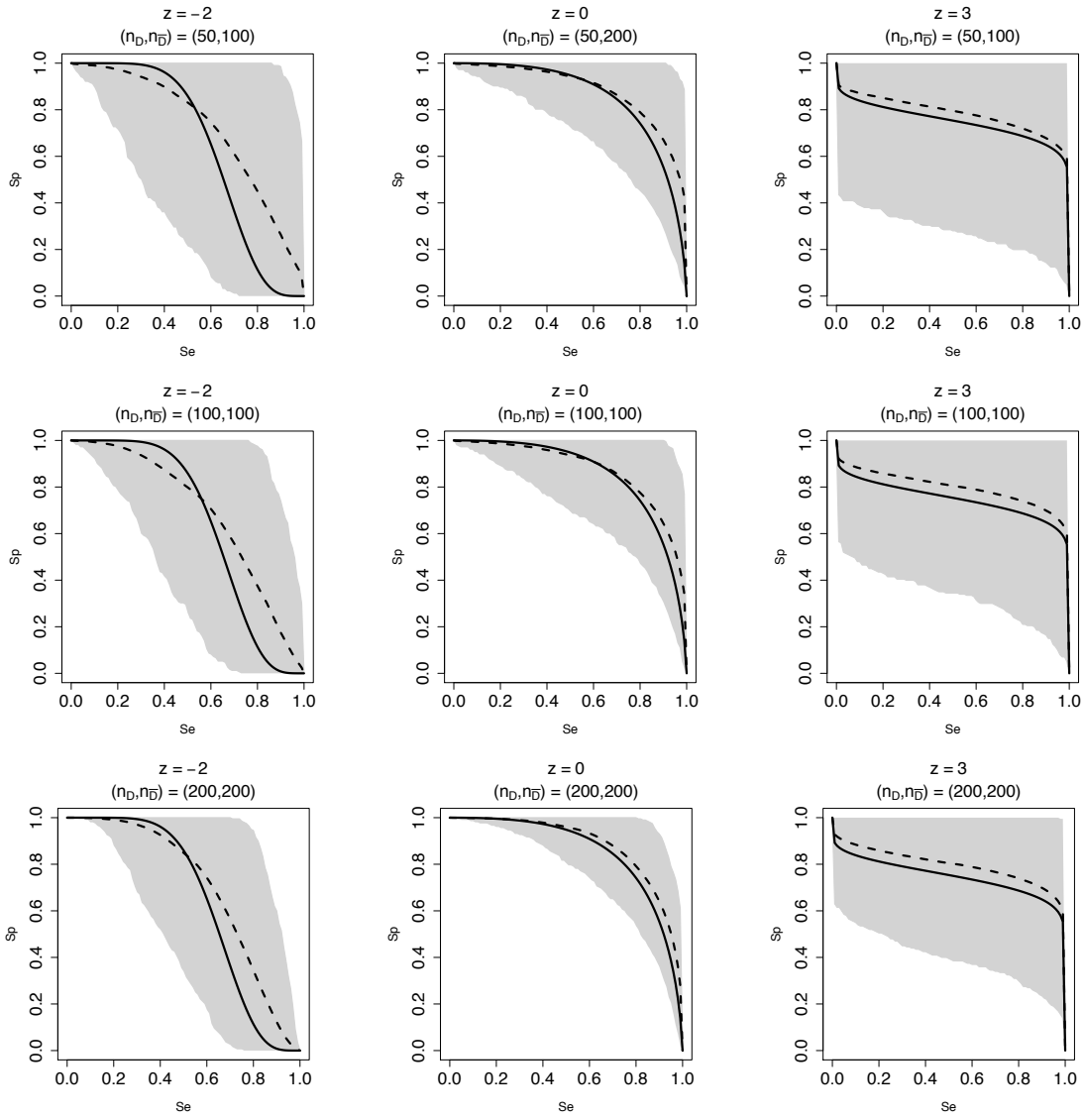

FIG 16. *Results for Scenario 3. True ROC_{Sp} curve (solid line) versus the mean of Monte Carlo estimates (dashed line) along with* 2.5% *and* 97.5% *simulation quantiles (gray area) for* $z = -2, 0,$ *and* 3.

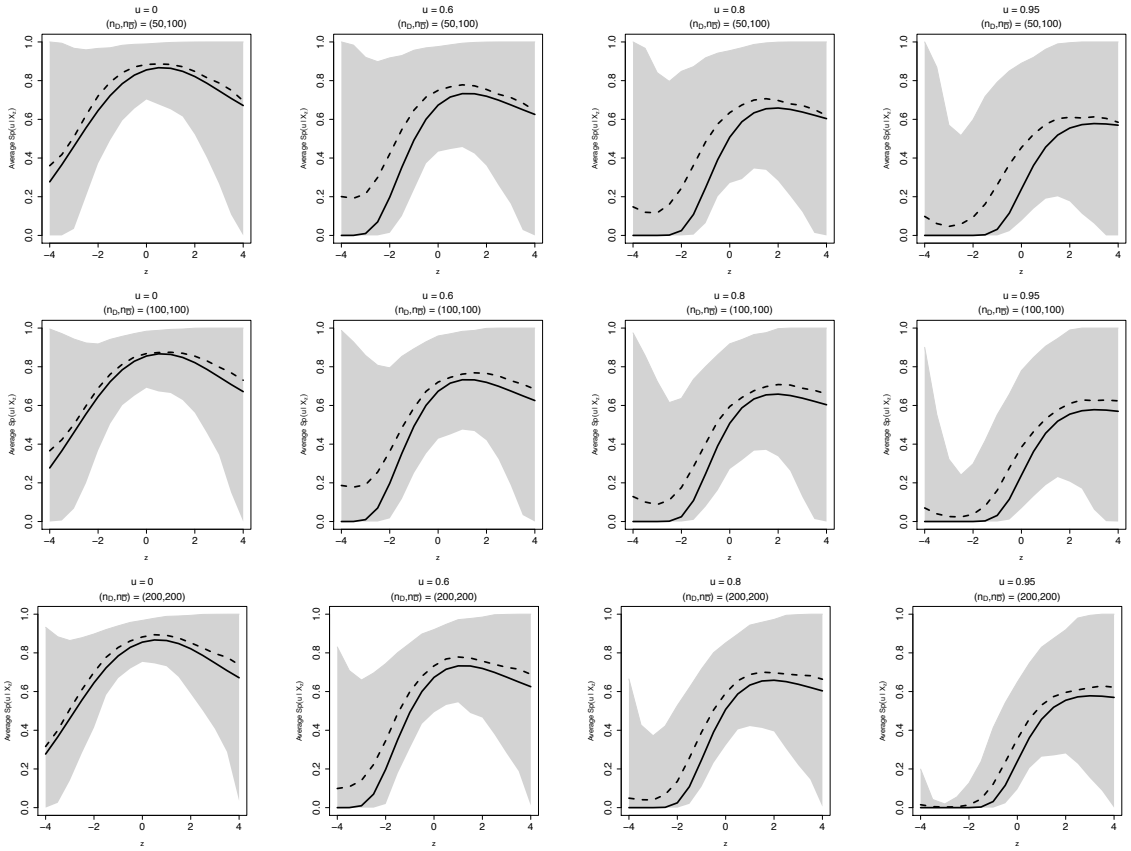

FIG 17. *Results for Scenario 3. True functional covariate-adjusted average specificity (solid line) versus the mean of Monte Carlo estimates (dashed line) along with* 2.5% *and* 97.5% *simulation quantiles (gray area) for* $u = 0, 0.6, 0.8,$ *and* 0.95.

Results for Scenario 4

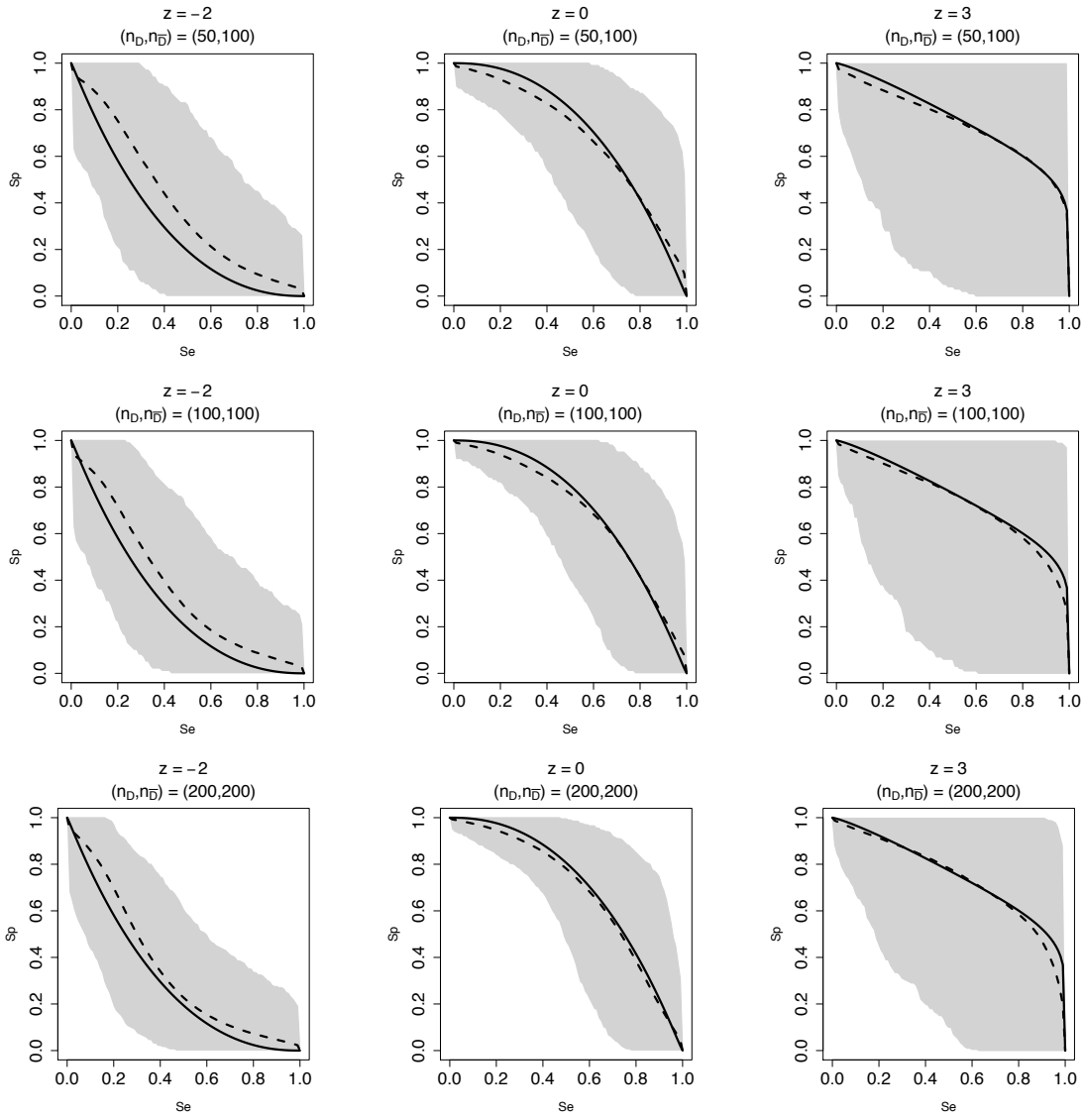

FIG 18. *Results for Scenario 4. True ROC_{Sp} curve (solid line) versus the mean of Monte Carlo estimates (dashed line) along with* 2.5% *and* 97.5% *simulation quantiles (gray area) for* $z = -2, 0,$ *and* 3.

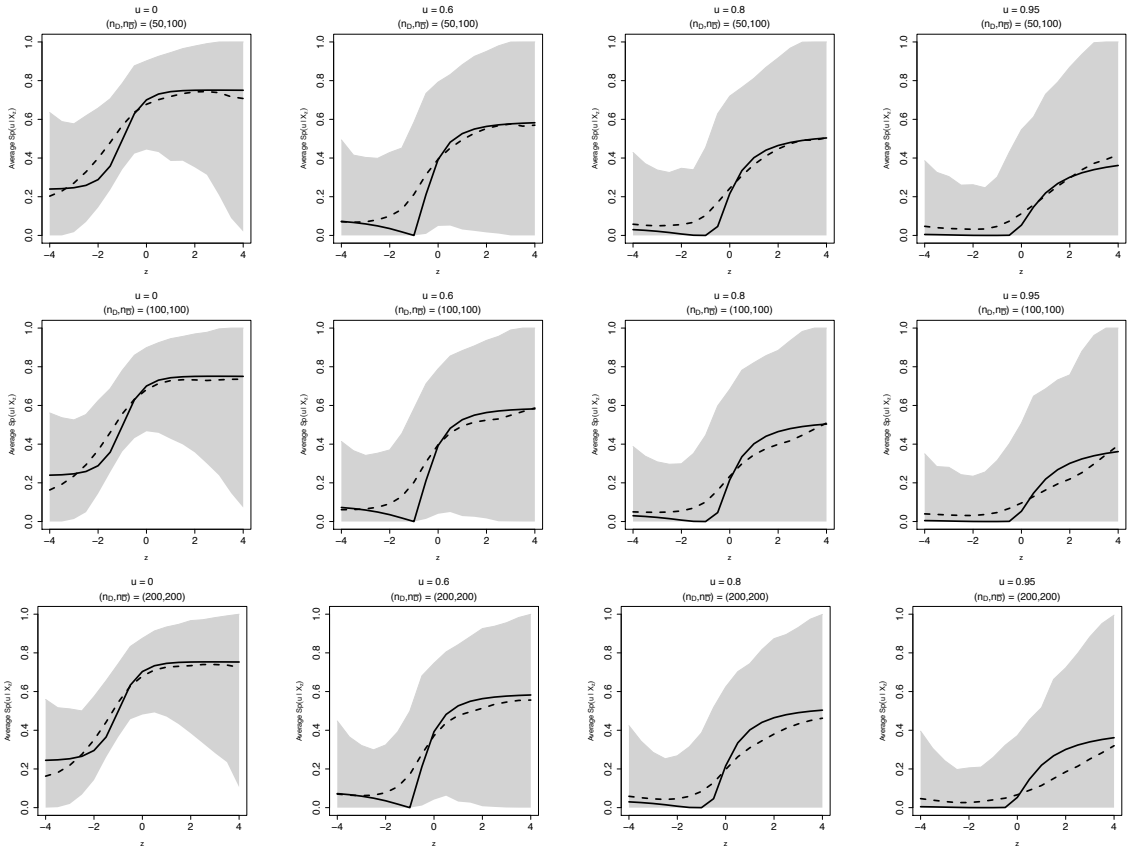

FIG 19. *Results for Scenario 4. True functional covariate-adjusted average specificity (solid line) versus the mean of Monte Carlo estimates (dashed line) along with* 2.5% *and* 97.5% *simulation quantiles (gray area) for* $u = 0, 0.6, 0.8,$ *and* 0.95.

```r
## R CODE FOR IMPLEMENTING OUR ESTIMATOR: A SIMULATED DATA EXAMPLE
## install.packages("fda.usc")
require(fda.usc)

## 1) TRUE VALUES
## Compute the true values of the functional covariate-adjusted pAUC
t <- seq(0, 1, by = 0.02)
nt <- length(t)

phi1 <- phi2 <- mu <- numeric(nt)

for(i in 1:nt) {
   phi1[i] <- sqrt(2) * sin(0.5 * pi * t[i])
   phi2[i] <- sqrt(2) * sin(1.5 * pi * t[i])
   mu[i] <- t[i] + sin(t[i])
}

phi1fd <- fdata(phi1, argvals = t)
phi2fd <- fdata(phi2, argvals = t)
beta <- phi1 + phi2
betafd <- fdata(beta, argvals = t)

lambda1 <- 4
lambda2 <- 1
z <- seq(-2 * sqrt(lambda1), 2 * sqrt(lambda1), by = 0.5)
nz <- length(z)

grid <- matrix(0, nrow = nz, ncol = nt)
for(j in 1:nz) {
  for(i in 1:nt) {
     grid[j, i] <- mu[i] + z[j] * phi1[i]
  }
}
gridfd <- fdata(grid, argvals = t)

rocspt <- function(p, j) {
    rocspt <- pnorm((3 + 1.5 * inprod.fdata(betafd, gridfd[j, ]) -
                     1.5 - inprod.fdata(betafd, gridfd[j, ])) + 2 *
                    qnorm(1 - p))
}
u <- 0
pauct <- numeric(nz)
for(j in 1:nz)
   pauct[j] <- integrate(rocspt, j = j, lower = u, upper = 1)$value
```

```r
## 2) SIMULATE DATA
## Settings for simulating data
nsim <- 1000; nd <- 100; nnd <- 100

## Simulate covariate curves
Xd <- array(0, c(nd, nt, nsim))
Xnd <- array(0, c(nnd, nt, nsim))
Xdfd <- Xndfd <- list()

set.seed(123)
for(j in 1:nsim) {
  Sigma <- exp(-0.2 * abs(outer(t, t, "-")))
  XGd <- mvrnorm(nd, mu = rep(0, nt), Sigma)
    for(i in 1:nd) {
        Xd[i,, j] <- mu + XGd[i, ] + rnorm(1, 0, sqrt(lambda1)) *
            phi1 + rnorm(1, 0, sqrt(lambda2)) * phi2
    }
  XGnd <- mvrnorm(nnd, mu = rep(0, nt), Sigma)
    for(l in 1:nnd) {
        Xnd[l,, j] <- mu + XGnd[l, ] + rnorm(1, 0, sqrt(lambda1)) *
            phi1 + rnorm(1, 0, sqrt(lambda2)) * phi2
     }
  Xdfd[[j]] <- fdata(Xd[,, j], argvals = t)
  Xndfd[[j]] <- fdata(Xnd[,, j], argvals = t)
}

## Simulate responses
yd <- epsd <- matrix(0, nrow = nd, ncol = nsim)
ynd <- epsnd <- matrix(0,nrow=nnd,ncol = nsim)

for(j in 1:nsim) {
    epsd[, j] <- rnorm(nd, 0, 1)
    epsnd[, j] <- rnorm(nnd, 0, 1)
    for(i in 1:nd) {
        yd[i, j] <- 3 + 1.5 * inprod.fdata(betafd, Xdfd[[j]][i, ]) +
            2 * epsd[i, j]
    }
    for(l in 1:nnd) {
        ynd[l, j] <- 1.5 + inprod.fdata(betafd, Xndfd[[j]][l, ]) + epsnd[l, j]
    }
}
```

```
## 3) IMPLEMENT OUR ESTIMATOR
regremd <- regremnd <- regvd <- regvnd <- list()
md <- zd <- vd <- resd <- matrix(0, nrow = nd, ncol = nsim)
mnd <- znd <- vnd <- resnd <- matrix(0, nrow = nnd, ncol = nsim)
mdz <- vdz <- mndz <- vndz <- matrix(0, nrow = nz, ncol = nsim)
ydws <- array(0, c(nd, nz, nsim))
yndws <- array(0, c(nd, nz, nsim))

for(j in 1:nsim) {
    regremd[[j]] <- fregre.np.cv(Xdfd[[j]], yd[,j], Ker = AKer.norm,
                                 metric = metric.lp, type.CV = "GCV.S",
                                 type = "S.NW")
    md[, j] <- regremd[[j]]$fitted.values
    zd[, j] <- (yd[, j] - md[, j])^2
    regvd[[j]] <- fregre.np.cv(Xdfd[[j]], zd[,j], Ker = AKer.norm,
                               metric = metric.lp, type.CV = "GCV.S",
                               type = "S.NW")
    vd[, j] <- regvd[[j]]$fitted.values
    resd[, j] <- (yd[, j] - md[, j])/sqrt(vd[, j])
    regremnd[[j]] <- fregre.np.cv(Xndfd[[j]], ynd[,j], Ker = AKer.norm,
                                  metric = metric.lp, type.CV = "GCV.S",
                                  type = "S.NW")
    mnd[, j] <- regremnd[[j]]$fitted.values
    znd[, j] <- (ynd[, j] - mnd[, j])^2
    regvnd[[j]] <- fregre.np.cv(Xndfd[[j]],znd[, j], Ker = AKer.norm,
                                metric = metric.lp, type.CV = "GCV.S",
                                type = "S.NW")
    vnd[, j] <- regvnd[[j]]$fitted.values
    resnd[, j] <- (ynd[, j] - mnd[, j]) / sqrt(vnd[, j])
    mdz[, j] <- predict.fregre.fd(regremd[[j]], gridfd)
    vdz[, j] <- predict.fregre.fd(regvd[[j]], gridfd)
    mndz[, j] <- predict.fregre.fd(regremnd[[j]], gridfd)
    vndz[, j] <- predict.fregre.fd(regvnd[[j]], gridfd)
    for(i in 1:nz) {
        ydws[, i, j] <- mdz[i, j] + sqrt(vdz[i, j]) * resd[, j]
        yndws[, i, j] <- mndz[i, j] + sqrt(vndz[i, j]) * resnd[, j]
    }
}

survivald <- function(yd, obs) {
  nd <- length(yd)
  estimate <- sum(yd > obs) / nd
}

aux <- array(0, c(nnd, nz, nsim))
```

```
pauc <- matrix(0, nrow = nz, ncol = nsim)
for(k in 1:nsim) {
  for(j in 1:nz) {
    for(i in 1:nnd) {
        aux[i, j, k] <- max(u, survivald(ydws[, j, k],yndws[i, j, k]))
    }
    pauc[j, k] <- (1 / nnd) * sum(aux[, j, k]) - u
  }
}

paucl <- paucm <- pauch <- numeric(nz)
for(j in 1:nz) {
  paucl[j] <- quantile(pauc[j, ], 0.025)
  paucm[j] <- mean(pauc[j, ])
  pauch[j] <- quantile(pauc[j, ], 0.975)
}
```

6. `R` code for implementing our estimator. The `R` code above illustrates how to implement our estimator on a simulated data example. After running the code we obtain the following estimates:

```
paucm
```

```
##  [1] 0.5395841 0.5826296 0.6261810 0.6676166 0.7070899 0.7429569 0.7768402
##  [8] 0.8090204 0.8371998 0.8620186 0.8846186 0.9039986 0.9194026 0.9320457
## [15] 0.9432305 0.9522996 0.9576184
```

These values should be compared with the true values of the functional covariate-adjusted pAUC (`pauc`) over the selected grid (`grid`), that is:

```
pauct
```

```
##  [1] 0.4994792 0.5439928 0.5879604 0.6308497 0.6721682 0.7114793 0.7484165
##  [8] 0.7826924 0.8141040 0.8425336 0.8679448 0.8903763 0.9099318 0.9267685
## [15] 0.9410844 0.9531060 0.9630756
```

REFERENCES

González-Manteiga, W., Pardo-Fernández, J. C. and Van Keilegom, I. (2011). ROC curves in non-parametric location–scale regression models. *Scand. J. Statist.* **38** 169–184.

Hall, P. G. and Hyndman, R. J. (2003). Improved methods for bandwidth selection when estimating ROC curves. *Statist. Prob. Lett.* **64** 181–189.

Lloyd, C. J. (1998). Using smoothed receiver operating characteristic curves to summarize and compare diagnostic systems. *J. Amer. Statist. Assoc.* **93** 1356–1364.

Yao. F., Fu, Y. and Lee, T. C. M. (2011). Functional mixture regression. *Biostatistics* **12** 341–353.

Vanda Inácio de Carvalho, Miguel de Carvalho
Faculty of Mathematics
Pontificia Universidad Católica de Chile
Av. Vicuña Mackenna, 4860, Santiago, Chile
E-mail: vanda.kinets@gmail.com
E-mail: mmbbcarvalho@gmail.com

Todd Alonzo
Department of Preventive Medicine
University of Southern California
440 E. Huntington Dr. Arcadia, CA 91006, USA
E-mail: talonzo@childrensoncologygroup.org

Wenceslao González-Manteiga
Department of Statistics and Operations Research
University de Santiago de Compostela
15782 Santiago de Compostela, Spain
E-mail: wenceslao.gonzalez@usc.es